HHS Public Access

Author manuscript

Nat Neurosci. Author manuscript; available in PMC 2013 March 01.

Published in final edited form as:

Nat Neurosci. 2012 September ; 15(9): 1192–1194. doi:10.1038/nn.3190.

Experience-dependent regulation of NG2 progenitors in the developing barrel cortex

Jean-Marie Mangin[1,2,*], **Peijun Li**[1], **Joseph Scafidi**[1], and **Vittorio Gallo**[1,*]

[1]Center for Neuroscience Research, Children's National Medical Center, 111 Michigan Ave, NW, Washington, DC 20010-2970, USA

[2]INSERM URMS 952, CNRS UMR 7224, 7 Quai Saint Bernard, 75252 Paris, Université Pierre et Marie Curie, Paris, France

Abstract

We show that during formation of the mouse barrel cortex, NG2 cells receive glutamatergic synapses from thalamocortical fibers and preferentially accumulate along septa separating the barrels. Sensory deprivation reduces thalamocortical inputs on NG2 cells and increases their proliferation, leading to a more uniform distribution within the deprived barrels. Therefore, early sensory experience regulates thalamocortical innervation on NG2 cells, as well as their proliferation and distribution during development.

Keywords

Oligodendrocyte progenitors; somatosensory cortex; barrel fields

NG2-expressing oligodendrocytes progenitor cells (NG2 cells) represent the largest population of neural progenitors in the developing postnatal and adult brain[1]. NG2 cells receive functional glutamatergic synapses[2] whose function is unknown. Because NG2 cells are still able to proliferate and migrate while receiving functional synapses[3-5], it has been proposed that neuron-NG2 cell synapses could regulate NG2 cell development in an activity-dependent manner[2]. To define the role of neuron-NG2 cell synapses in a physiological system, we investigated functional and developmental interactions between thalamocortical axons and NG2 cells in the mouse somatosensory cortex.

We performed patch-clamp recordings in thalamocortical slices from CNP-EGFP mice between 3 and 5 postnatal days (3–5PND; Supplementary Fig. 1). Ventrobasal stimulation

*Correspondence should be addressed to: Dr. Jean-Marie Mangin, INSERM URMS 952, CNRS UMR 7224, 7 Quai Saint Bernard, Bat B2, 75252 Paris cedex 05, Université Pierre et Marie Curie, Paris, France. Tel: +33 1 44 27 25 19, jean-marie.mangin@inserm.fr, Dr. Vittorio Gallo, Center for Neuroscience Research, Children's National Medical Center, Room M7643, 111 Michigan Ave., NW, Washington, DC 20010, Phone: 202-476-4996, Fax: 202-476-4988, vgallo@cnmcresearch.org.

AUTHOR CONTRIBUTIONS

J.M. Mangin designed, performed and analyzed all experiments. P.J. Li and J. Scafidi performed and analyzed the dark rearing experiments. V. Gallo participated in the design of the experiments, supervised the whole project and wrote the manuscript with J.M. Mangin.

evoked excitatory postsynaptic currents (eEPSCs) in layer IV CNP-EGFP$^+$NG2$^+$ cells with average amplitude and decay time of 48 ± 82 pA and 1.6 ± 0.3 ms, respectively (n=16 cells) (Fig. 1a). The average stimulation-to-response delay was 6.8 ± 0.4 ms (n = 16 cells) as expected for unmyelinated thalamocortical fibers[6]. eEPSCs were blocked by the AMPA-receptor antagonist CNQX (10 μM; n=5 cells; Fig. 1b). Serotonin (5-HT) inhibits presynaptic release of glutamate in synapses between thalamocortical axons from the ventrobasal nucleus and layer IV cortical neurons[7]. 20 μM 5-HT inhibited eEPSCs in layer IV CNP-EGFP$^+$NG2$^+$ cells by 63 ± 7 % (n = 5 cells) (Fig. 1c and d), but had no effects on AMPAR-mediated currents evoked by application of 1mM glutamate (Supplementary Fig. 2). These results confirm that EPSCs evoked in NG2 cells by ventrobasal stimulation depend on the synaptic release of glutamate from thalamocortical axons[7].

We investigated the distribution of CNP-EGFP$^+$NG2$^+$ cells in somatosensory cortex layer IV (Fig. 1e-f and Supplementary Fig. 3). At 6PND, barrels are structurally well defined, with a central core of VGLUT2$^+$ thalamocortical synapses, surrounded by a divider of NeuN$^+$ neurons[8]. Glutamine synthetase$^+$ astrocytes are accumulated in barrel cores[9]. CNP-EGFP$^+$NG2$^+$ cells exhibited a low density in barrel cores, but accumulated in septa separating neurons likely belonging to different barrels. This distribution was observed by intensity profile plot and cell counting perpendicular to barrel walls (Supplementary Fig. 3). The specific distribution of CNP-EGFP$^+$NG2$^+$ cells was detectable as soon as barrels emerged around 4PND (Supplementary Fig. 4). At 2PND, we could already detect a specific decrease in CNP-EGFP- and NG2-associated immunofluorescence in emerging layer IV and layer VI of the somatosensory cortex, where thalamocortical axons begin to accumulate[10] (Supplementary Fig. 5). The layer specific distribution of NG2 could still be observed at 15PND (Supplementary Fig. 6), while a large number of oligodendrocytes were myelinating.

Early sensory experience is known to regulate barrel formation[11] but its influence on NG2 cells has never been investigated. We removed and cauterized the central row (C row) of mystacial whiskers at birth and analyzed NG2 cell distribution in the barrels corresponding to deprived whiskers (Fig. 2a-e). At 6PND, the distribution of CNP-EGFP$^+$NG2$^+$ cells was more uniform in the C row barrels of deprived animals, as compared to controls; CNP-EGFP$^+$NG2$^+$ cell density increased by 26 ± 6 % (n = 4 animals, $p<0.05$), and average fluorescence intensity for CNP-EGFP and NG2 were both higher in deprived barrel row C, as compared to surrounding barrel row B and D ($p<0.001$).

We performed a deprivation of all whiskers on the right side whisker pad at birth and compared the density of CNP-EGFP$^+$NG2$^+$ cells in all layers between the control hemisphere ipsilateral to the lesion - where the intact whiskers are represented - and the deprived hemisphere contralateral to the lesion - where the deprived whiskers are represented (Fig. 2f). The density of CNP-EGFP$^+$NG2$^+$ cells was increased by 34.9 ± 7.3 % in layer IV of the deprived hemisphere (36,360 ± 1750 cells by mm^3), as compared to the control hemisphere (27,200 ± 1100 cells by mm^3, n = 4 animals; paired t-test; $p<0.01$). Density in layer II-III (control = 30,400 ± 800 and deprived = 29,800 ± 1100 cells by mm^3) and V (control = 38,700 ± 1200 and deprived = 37,100 ± 1300 cells by mm^3) was not

significantly affected, and a small increase in layer VI failed to reach significance (control = 29,800 ± 1200 and deprived = 32,600 ± 1500 cells by mm^3).

We then determined whether the strength of thalamocortical glutamatergic inputs onto layer IV NG2 cells could vary according to location of these cells within the barrel, and whether these inputs could be regulated by early sensory deprivation. We compared the glutamatergic innervation of layer IV CNP-EGFP$^+$NG2$^+$ cells at 4–5PND in the barrel cores and septa of control barrel cortex with the innervation of layer IV CNP-EGFP$^+$NG2$^+$ cells of deprived barrel cortex. To minimize the variability in evoked EPSC amplitudes, we recorded glutamatergic EPSCs in layer IV CNP-EGFP$^+$NG2$^+$ cells in response to stimulation of the subcortical white matter (SCWM) below each recorded cell. EPSCs evoked in CNP-EGFP$^+$NG2$^+$ cells were blocked by CNQX and inhibited by 20 μM 5-HT (57 ± 12 %; n = 4 cells), confirming that at this age they mostly arise from thalamocortical glutamatergic axons. The average amplitude of evoked EPSCs was significantly higher in layer IV CNP-EGFP$^+$NG2$^+$ cells located in barrel cores (93.2 ± 78.7 pA; n = 8 cells) than in cells located in septa (9.7 ± 8.3 pA; n = 9 cells; $p<0.01$), or in layer IV CNP-EGFP$^+$NG2$^+$ cells recorded in the deprived side (20.1 ± 17.8 pA; n=8 cells; $p<0.05$) (Fig. 3a-e). We also determined how C row deprivation alone would affect the strength of TC input in CNP-EGFP$^+$NG2$^+$ cells located in the deprived C row barrel cores and in cells located in the septa surrounding the deprived row, as compared to surrounding control barrels septa and cores. We used a slice preparation across barrel row A to E, which allows identifying each row of barrels individually[12] (see Supplementary Fig. 7a and 7b). While we found that CNP-EGFP$^+$NG2$^+$ cells located in deprived barrel C core received significantly weaker inputs (38.3 ± 22.3 pA; n=8 cells, Supplementary Fig. 7b) than cells located in surrounding barrel cores (108.1 ± 78.5; n=10 cells; $p<0.05$), we did not see any significant differences between cells located in septa separating control barrels (14.2 ± 12.7 pA; n=9 cells) and septa separating deprived and non-deprived barrels (16.6 ± 13.0 pA; n=9 cells; $p>0.05$), with the average input strength remaining low in both cases.

Differences in the strength of thalamocortical innervation detected between these distinct groups of CNP-EGFP$^+$NG2$^+$ cells correlated with differences in their proliferation rate. We performed dual immunostaining for Ki67, a marker of proliferating cells, and VGLUT2 to visualize barrel cores in 4PND CNP-EGFP mice, and analyzed CNP-EGFP$^+$ cell proliferation. At this age, virtually all CNP-EGFP$^+$ cells are NG2$^+$ (>95%, see Fig. 1). The proliferation rate of CNP-EGFP$^+$ cells was significantly higher in barrel septa (27.3 ± 1.9 %) than in barrel cores (19.5 ± 1.3 %; n = 3 animals, paired t-test $p<0.05$) (Fig. 3f-g). By comparing the percentage of CNP-EGFP$^+$ cells expressing Ki67 in the somatosensory cortex between control and deprived hemisphere at 3PND, we found that this was significantly increased in the deprived hemisphere (21.8 ± 3.2 %), as compared to the control hemisphere (16.3 ± 0.9 %; n=4 animals paired t-test $p<0.05$) (Fig. 3h-k).

In order to analyze a different sensory system, we investigated the distribution of NG2 cells in the primary visual cortex during development and after dark rearing. NG2 cells exhibited a lower density in layer 4 of the visual cortex (Supplementary Fig. 8). However, this decrease appeared at least two weeks later than in the somatosensory cortex, as it was detectable at P14 using intensity profile plot, but only around P21 by cell counting. Visual

deprivation using a dark rearing protocol did not alter NG2 cell distribution and density (Supplementary Fig. 9).

We show that NG2 cells in cortical layer IV receive glutamatergic synapses from somatosensory thalamocortical axons during formation of the barrel cortex. As thalamocortical fibers start innervating their target areas in cortical layer IV and VI around 2PND, NG2 cells tend initially to be excluded from these layers, but subsequently accumulate in the septa separating layer IV barrels as they emerge around 4PND. This partially results from a higher proliferation rate of NG2 cells in the septa - where they receive weaker thalamocortical inputs - than in barrel cores - where they are more strongly innervated by thalamocortical axons. The specific location of NG2 cells, their proliferation rate and their innervation by thalamocortical fibers all depend on normal sensory experience after birth. While the location and proliferation rate of NG2 cells may not be directly regulated by their thalamocortical innervation, but due to a secondary effect of this innervation, our results are consistent with previous findings demonstrating that glutamate inhibits NG2 cell proliferation and promotes their migration[13,14]. Changes in glutamate-induced proliferation and motility - combined with distinct effects on NG2 cell proliferation in barrel cores and septa - could lead to the preferential accumulation of NG2 cells in barrel septa. Since adult barrel septa are more heavily myelinated than barrel cores[15] and sensory deprivation abolishes the distribution of myelinated fibers[15], experience-dependent regulation of NG2 accumulation could constitute one of the mechanisms that control the number and positioning of myelinated fibers in the adult somatosensory cortex.

METHODS

Materials

The CNP-EGFP mouse has been described previously[16]. Animal procedures complied with National Institutes of Health and Children's Research Institute guidelines. All reagents were from Sigma (St. Louis, MO), unless otherwise stated; CNQX, QX-314, SR 95531 (gabazine) were from Tocris Cookson Ltd. (Ellisville, MO). Primary antibodies were: anti-NG2 (rabbit, 1:200), anti-NeuN (mouse, 1:500), anti-VGLUT2 (rabbit, 1:200) from Chemicon (Temecula, CA), anti-Glutamine synthetase (rabbit, 1:200) from Abcam, anti-Ki67 (rabbit, 1:500) from Novocastra (Newcastle, UK) and anti-parvalbumin (rabbit, 1:2000) from Swant (Switzerland). Secondary antibodies (1:200) were from Jackson ImmunoResearch Laboratories, Inc.

Immunocytochemistry and confocal microscopy

Biocytin-filled, patch-clamp-recorded CNP-EGFP$^+$ cells were visualized by fluorescence microscopy in brain slices and underwent immunocytochemical characterization with anti-NG2[17]. CNP-EGFP mice at 2-28 PND were anesthetized with isofluorane, intracardially perfused with 4% paraformaldehyde, and brains were removed. Dark reared mice (n = 11) had their eyes covered throughout the anesthetization and perfusion procedures. Tangential, thalamocortical and coronal tissue sections (50–100 μm) were prepared using a vibratome (floating sections) and immunostained[17]. Images were acquired using a Zeiss LSM 510 (Zeiss, Jena, Germany). For all images, *z*-sections and *z*-steps ranged between 2 and 3 μm,

respectively. Images were processed using ImageJ (NIH) and Adobe Illustrator (Adobe Systems, San Jose, CA).

Cell counting and fluorescence profile plot

To measure the density of CNP-EGFP$^+$NG2$^+$ OPCs and GS$^+$ astrocytes, we counted the number of CNP-EGFP$^+$ or GS$^+$ soma co-localizing with DAPI nuclear staining in confocal z-stack (30 μm thickness; z-step=2μm) in the region of interest (ROI: barrel row, cortical layer, etc.). Densities were obtained by dividing the number of cells counted by the volume of the ROI (surface of the section analyzed × thickness = 30 μm), and expressed in number of cells by mm^3. The surface analyzed was identical between conditions (control and after deprivation).

To quantify the density of CNP-EGFP$^+$NG2$^+$, NeuN$^+$ neurons and GS$^+$ astrocytes across barrel walls, we aligned barrels as vertically as possible based on DAPI staining, and then measured the x coordinate of each type of cells by using the same rectangular ROI for each barrel wall. Measurements were limited to a group of smaller barrels representing the small frontal whiskers and exhibiting a similar diameter and circular/hexagonal shape. Measurement were made separately for group of cells across each barrel wall and then pooled together. X coordinates were plotted for each section analyzed (bin size = 5 μm). Relative densities were obtained by dividing the number of cells for each bin by the total number of cell counted in the ROI. Density values were express as percentages, with 100% being the sum of all bins. Final histograms represent the average of normalized density distribution histograms from 3 different animals.

Fluorescence intensity profile plots were obtained using the "*plot profile*" in ImageJ (NIH). We either show individual or average image profile plots at a single pixel resolution, or average profile plots in which intensity value of several adjacent pixels are averaged (9-10 pixel per bin).

Slice preparation

Brain hemispheres were dissected from 3-5PND CNP-EGFP mice on ice and cut into 500-μm thick thalamocortical sections on a Leica VT1000S vibratome, then placed in an ice cold oxygenated solution (in mM): 87 NaCl, 2.5 KCl, 1.25 NaH2PO4, 7 MgCl2, 0.5 CaCl2, 25 NaHCO3, 25 glucose, 75 sucrose (347 mOsmol) at pH 7.4. Slices were stored in the same solution at 35°C for 30 min, then transferred into artificial cerebrospinal fluid (ACSF; in mM): 124 NaCl, 3 KCl, 2.5 CaCl2, 1.3 MgSO4, 26 NaHCO3, 1.25 NaHPO4, 15 glucose; saturated with 95% O2/5% CO2 at room temperature.

Patch-clamp recordings

Slices were transferred to a recording chamber and perfused with ACSF at a rate of 1-2 ml.s^{-1}. Patch electrodes had resistances between 3 and 6 MΩ when filled with an intracellular solution (in mM): 130 K-gluconate, 20 KCl, 2 MgCl, 0.1 EGTA, 10 HEPES, 0.4 Na-GTP, 2 Na-ATP and biocytin (3 mg/ml), solution adjusted to pH 7.3, 275 mOsm. Whole-cell recordings from CNP-EGFP$^+$ cells were obtained using a Multiclamp 700B (Molecular Devices, Sunnyvale, CA) and monitored via a PC running pClamp 9.2

(Molecular Devices). Barrel cores could be visualized by infrared videomicroscopy, based on their low light absorption compared to the surrounding tissue. Between 3 and 4PND, the region where TC fibers terminate could similarly be identified as a continuous band of cortex exhibiting a lower light absorption. Additionally, layer IV of the somatosensory cortex could be recognized based on its lower density in CNP-EGFP$^+$ cells compared to layer V and III. The exact anatomical location of each recorded cells was determined after patch-clamp recording by defining the position of the patch pipette tip relative to the low light absorption territories corresponding to barrel cores on the control sides, or relative to the continuous layer of TC fibers before 4 PND, or in deprived side. Cells that were recorded in the incorrect layers - mostly upper layer V and lower layer III - were routinely discarded. The cellular and physiological identity of the recorded EGFP$^+$ cells was routinely confirmed by: i) using current-voltage steps to test for the presence of transient inward K^+ current upon depolarization, and ii) filling all cells with biocytin during patch-clamp recording, followed by labeling with anti-NG2 antibodies and biocytin. The Ventro-basal (VB) nucleus or SCWM were stimulated using small bipolar electrodes (FHC, Bowdoin, ME). Stimulations were performed at a low frequency (0.07 Hz), in order to evoke a stable response. For each slice, in order to identify the region of the barrel cortex that was still functionally connected to the VB thalamic nucleus, we first performed extracellular current recordings at different locations in response to VB stimulation. The region connected by mono-synaptic thalamocortical synapses specifically exhibited a transient hyperpolarization 6-7 ms after VB stimulation, a delay expected for unmyelinated TC fibers at this age. Field potential recordings were obtained by using a glass electrode (tip resistance ≈ 0.5 MΩ) filled with ACSF and connected to a multiclamp 700B amplifier (Axon Instruments, USA). While VB stimulation was used to demonstrate without ambiguity that NG2 cells are innervated by TC fibers from the VB somatosensory cortex, this method could not be reliably used to quantify and compare the degree of innervation of layer IV NG2 cells. In a given slice, the amplitude of EPSCs evoked by VB stimulation mostly depends on the number of TC axons that are preserved in the slice preparation and that are able to propagate an action potential from the VB to the somatosensory cortex. As the number of preserved axons greatly varies between different slices - as well as between adjacent barrels – comparing data of VB stimulation in separate slices, or even between different barrels in the same slice, would result in a high degree of variability in the amplitude of evoked EPSCs. To minimize the variability in evoked EPSC amplitudes when comparing TC inputs between different groups of layer IV NG2 cells, we recorded their response to a stimulation of the subcortical white matter (SCWM) below each recorded cell. Pulses were generated using pClamp 9.2 (Molecular Devices) and applied with a constant current stimulus isolator (DS3, Digitimer Ltd., Hertfordshire, England). The stimuli used to elicit evoked EPSCs varied between 10 and 500 μA in intensity, and were 100 μs in duration. Average EPSC amplitudes were calculated by averaging 20-50 responses to a maximal intensity stimulus (500 μA/100 μs). Field potential recordings were obtained by using a glass electrode (tip resistance ≈ 0.5 MΩ) filled with ACSF and connected to a multiclamp 700B amplifier (Axon Instruments, USA). Each of the different drugs was applied via the bath solution. Off-line analysis was performed using Clampfit 9.2 (Molecular Devices) and Mini Analysis (Synaptosoft Inc., Fort Lee, NJ). In all experiments, data were filtered at 10 kHz during capacitance

compensation and 5 kHz during subsequent data recording. The traces were digitized at 10 kHz. All voltage measurements and steps were corrected for a junction potential offset.

Whisker cauterization

Whisker lesions were performed as described[11]. Neonatal mice were anesthetized by cooling and then kept on ice during the entire surgical procedure. The C row of facial whiskers was identified under a surgical microscope and, after plucking, whiskers were ablated with a surgical cautery device (Bovie, Clearwater, FL). After cauterization, the mice were revived, returned to their mothers, and sacrificed at the indicated time points.

Dark Rearing

Control group mice were raised in a normal lighted environment (12 hr on/12 hr off light cycle) and perfused at 7, 14, 21 and 28 PND. Dark reared mice were born and raised in complete darkness until 28 PND, with short periods of dim red light for animal husbandry. The efficiency of the dark rearing paradigm was confirmed by parvalbumin interneuron staining, which exhibited a lower density in the dark-reared group compared to control[18].

Statistical analysis

All statistical analysis was performed with unpaired t-test, or paired t-test when indicated. Results were deemed significantly different if $p < 0.05$.

Supplementary Material

Refer to Web version on PubMed Central for supplementary material.

Acknowledgments

We thank Drs. Dwight Bergles and Molly Huntsman for discussion. We thank Drs. Li-Jin Chew, Josh Corbin, Molly Huntsman and Judy Liu for critically reading an earlier version of this manuscript. We thank Dr. Elizabeth Quinlan (University of Maryland, College Park) for her advice on the dark rearing experiments. We also thank Drs. Ramesh Chittajallu and John Isaac for their help with the thalamocortical slice preparation. This work was supported by NIH R01NS045702, R01NS056427 and NIH IDDRC P30HD40677 (V.G.), by NIH K08NS073793 (J.S.), and by ANR JCJC Grant *Oligospine* (J.M.M.).

References

1. Dawson MR, Polito A, Levine JM, Reynolds R. MCN. 2003; 24:476–488. [PubMed: 14572468]
2. Mangin JM, Gallo V. ASN Neuro. 201110.1042/AN20110001
3. Kukley M, Kiladze M, Tognatta R, Hans M, Swandulla D, Schramm J, Dietrich D. FASEB J. 2008; 22:2957–69. [PubMed: 18467596]
4. Ge WP, Zhou W, Luo Q, Jan LY, Jan YN. PNAS. 2009; 106:328–33. [PubMed: 19104058]
5. Tanaka Y, Tozuka Y, Takata T, Shimazu N, Matsumura N, Ohta A, Hisatsune T. Cereb Cortex. 2009; 19:2181–95. [PubMed: 19131437]
6. Daw MI, Ashby MC, Isaac JT. Nat Neurosci. 2007; 10:453–61. [PubMed: 17351636]
7. Laurent A, Goaillard JM, Cases O, Lebrand C, Gaspar P, Ropert N. J Neurosci. 2002; 22:886–900. [PubMed: 11826118]
8. Erzurumlu RS, Kind PC. TINS. 2001; 24:589–95. [PubMed: 11576673]
9. Houades V, Koulakoff A, Ezan P, Seif I, Giaume C. J Neurosci. 2008; 28:5207–17. [PubMed: 18480277]

10. Erzurumlu RS, Jhaveri S. Brain Res Dev Brain Res. 1990; 56:229–34. [PubMed: 2261684]
11. Datwani A, Iwasato T, Itohara S, Erzurumlu RS. J Neurosci. 2002; 22:9171–5. [PubMed: 12417641]
12. Finnerty GT, Roberts LS, Connors BW. Nature. 1999; 22:367–71. [PubMed: 10432115]
13. Yuan X, Eisen AM, McBain CJ, Gallo V. Development. 1998; 125:2901–2914. [PubMed: 9655812]
14. Gudz TI, Komuro H, Macklin WB. J Neurosci. 2006; 26:2458–66. [PubMed: 16510724]
15. Jain N, Diener PS, Coq JO, Kaas. J Neurosci. 2003; 23:10321–30. [PubMed: 14614091]

ADDITIONAL REFERENCES

16. Yuan X, Chittajallu R, Belachew S, Anderson S, McBain CJ, Gallo V. J Neurosci Res. 2002; 70:529–545. [PubMed: 12404507]
17. Mangin JM, Kunze A, Chittajallu R, Gallo V. J Neurosci. 2008; 28:7610–7623. [PubMed: 18650338]
18. Sugiyama S, Di Nardo A, Aizawa S, Matsuo I, Volovitch M, Prochiantz A, Hensch T. Cell. 2008; 134:508–520. [PubMed: 18692473]

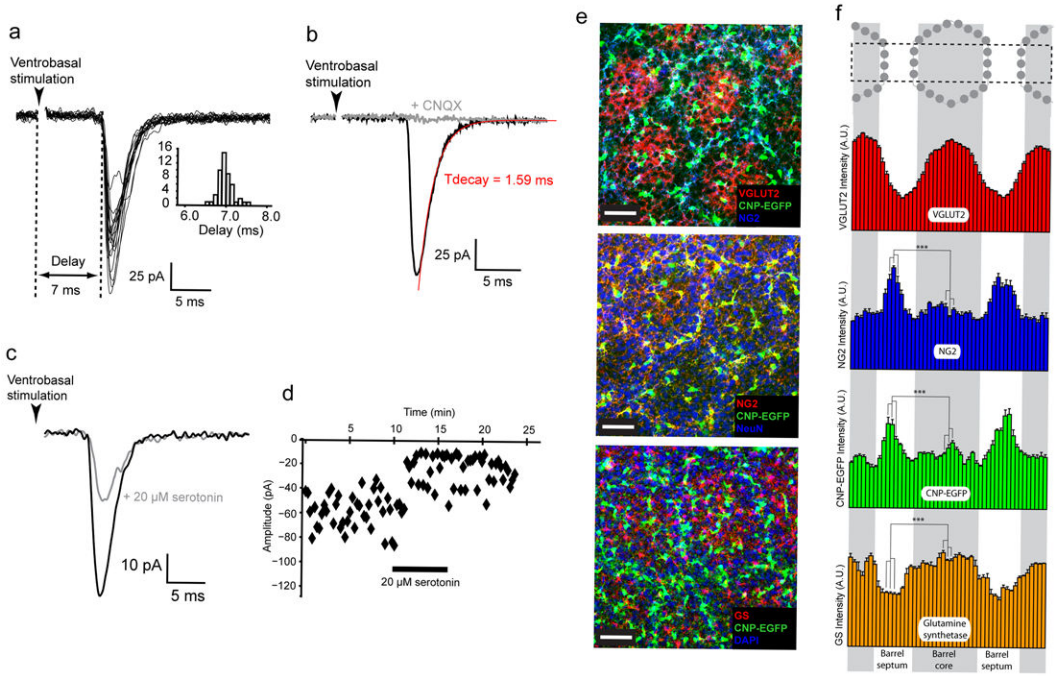

Figure 1. NG2$^+$ progenitors are functionally innervated by thalamocortical glutamatergic synapses and accumulate at the border between cortical barrels

(a) Stimulation of the VB nucleus evokes EPSCs in layer IV CNP-EGFP$^+$NG2$^+$ cells which exhibit a gaussian distribution of their delays (average delay = 7 ms). **(b-d)** EPSCs are blocked by 10 µM of CNQX and reduced by 20 µM serotonin. **(e)** Barrel field from 6PND CNP-EGFP mice immunostained for VGLUT2, NG2, NeuN and Glutamine Synthetase (GS). Scale bars = 50 µm **(f)** Average fluorescence intensity plots (n=3 animals, 3 barrel unit per animal, bin size = 5.5 µm) of VGLUT2, CNP-EGFP, NG2 and GS across barrels. Average NG2 and CNP-EGFP fluorescence were significantly more intense in barrel septa than in cores, while average GS fluorescence was significantly more intense in barrel cores (*** = p<0.001; error bars= s.e.m).

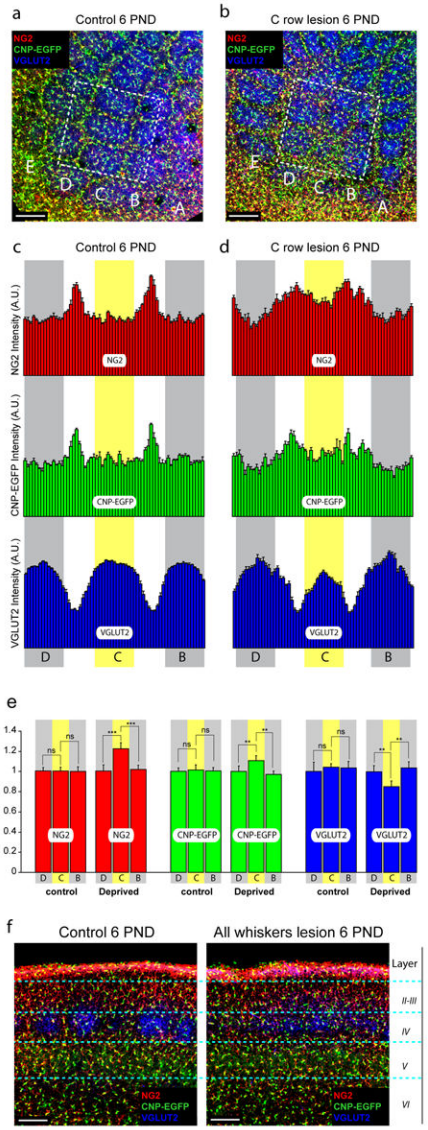

Figure 2. Whisker lesion at birth alters the density of NG2^{+} cells in the barrel fields

(a-b) Barrel fields in control (a) and C-row ablated (b) CNP-EGFP (green) transgenic mice at 6 PND immunostained for NG2 (red) and VGLUT2 (blue). Boxes delineate a region comprising the C row of whiskers and analyzed in panel c and d Scale bars = 200 μm. **(c-d)** Average fluorescence intensity plots (n=4 animals, bin size = 10 μm) showing the distribution of NG2, CNP-EGFP and VGLUT2 fluorescence across barrel rows under control conditions (c) and after C row deprivation (d). Control core regions in barrel row B and D are indicated in grey, while deprived core region in barrel C is indicated in yellow. **(e)** Normalized fluorescence intensities for NG2, CNP-EGFP and VGLUT2 in barrel row B, C and D under control conditions and after C row deprivation. After C row deprivation, NG2 and CNP-EGFP fluorescence were more intense in the C row core region than in surrounding B and D row core regions, while VGLUT2 intensity was lower (** = $p<0.01$; *** = $p<0.001$)(error bars = s.e.m.) **(f)** Hemi-coronal section of the barrel field from a 6PND

CNP-EGFP (green) mouse from control and deprived hemispheres immunostained for NG2 (red) and VGLUT2 (blue). Scale bars = 200 μm.

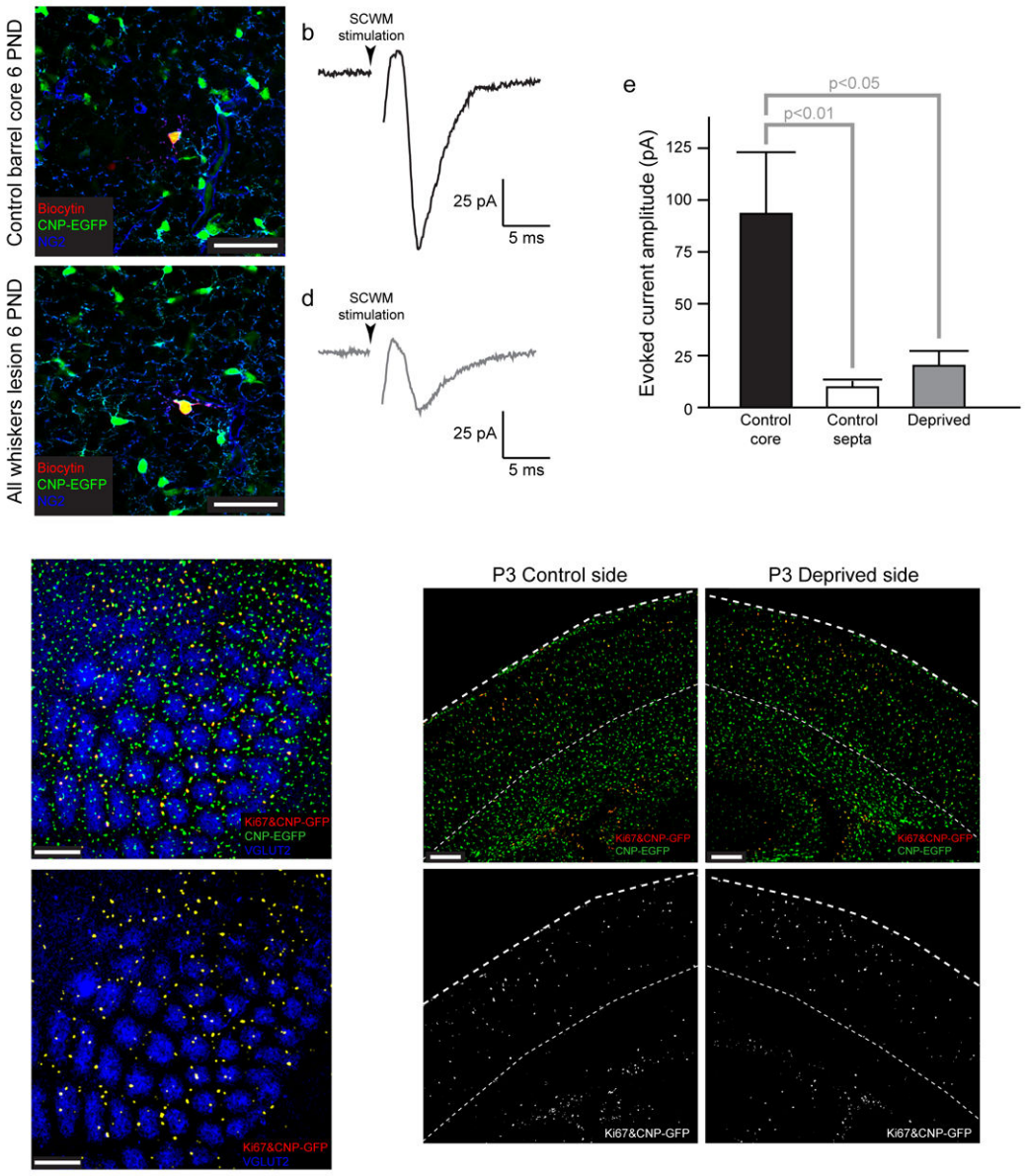

Figure 3. Location in the barrel field and sensory experience regulate the TC innervation and proliferation rate of NG2$^+$ progenitor cells

(a,c) Layer IV CNP-EGFP$^+$ cells recorded in the control (a) and deprived hemisphere (c) of a 4PND CNP-EGFP mouse. CNP-EGFP$^+$ cells (green) were filled with biocytin (red) and stained for NG2 (blue) Scale bars = 50 μm. **(b,d)** Average eEPSC evoked by SCWM stimulation in the cell shown in **a** (control, **b**), as compared to the cell shown in **c** (deprived, **d**). **(e)** Average amplitude of eEPSCs was higher in cells in barrel cores (93.2 ± 78.7 pA; n = 8 cells) than in septas (9.7 ± 8.3 pA; n = 9 cells; p<0.01) or in the deprived side (20.1 ± 17.8 pA; n=8 cells; error bars= s.e.m.). **(f)** Barrel field from a 4PND CNP-EGFP (green) mouse immunostained for Ki67 and VGLUT2. CNP-EGFP$^+$ and CNP-EGFP$^+$Ki67$^+$ cells are shown in the image. **(g)** Same image as in **f**, showing double labeled CNP-EGFP$^+$Ki67$^+$ cells (yellow) and VGLUT2 (blue). **(h-i)** Hemi-coronal section of the barrel field from a

3PND CNP-EGFP (green) mouse from control and deprived hemispheres immunostained for Ki67 (red). **(j-k)** Images showing only double labeled CNP-EGFP^{+}Ki67^{+} cells from the images shown in **h** and **i**. Scale bars = 200 μm